Geophysical Research Letters

RESEARCH LETTER
10.1029/2022GL100948

Northward Extent of Atmospheric Mercury Transboundary Transport to the Himalayas and Tibetan Plateau Region

Jie Huang[1,2], Shichang Kang[2,3], Xinbin Feng[4], Wenjun Tang[1,2], Kirpa Ram[5], Junming Guo[2,3], Qianggong Zhang[1,2], Chhatra Mani Sharma[6], Chaoliu Li[2,3], Lekhendra Tripathee[3], and Feiyue Wang[7]

[1]State Key Laboratory of Tibetan Plateau Earth System, Resources and Environment (TPESRE), Institute of Tibetan Plateau Research, Chinese Academy of Sciences, Beijing, China, [2]University of the Chinese Academy of Sciences, Beijing, China, [3]State Key Laboratory of Cryospheric Science, Northwest Institute of Eco-Environment and Resources, Chinese Academy of Sciences, Lanzhou, China, [4]State Key Laboratory of Environmental Geochemistry, Institute of Geochemistry, Chinese Academy of Sciences, Guiyang, China, [5]Institute of Environment and Sustainable Development, Banaras Hindu University, Varanasi, India, [6]Central Department of Environmental Science, Tribhuvan University, Kathmandu, Nepal, [7]Centre for Earth Observation Science, Department of Environment and Geography, University of Manitoba, Winnipeg, MB, Canada

Abstract Indian monsoon circulation is the primary driver of the long-range transboundary mercury (Hg) pollution from South Asia to the Himalayas and Tibet Plateau region, yet the northward extent of this transport remains unknown. In this study, a strong δ^{202}Hg signature overlapping was found between Lake Gokyo and Indian anthropogenic sources, which is an indicative of the Hg source regions from South Asia. Most of the sediment samples were characterized with relatively large positive Δ^{199}Hg values (mean = 0.07‰–0.44‰) and small positive Δ^{200}Hg values (mean = 0.03‰–0.08‰). Notably, the Δ^{199}Hg values in the lake sediments progressively increased from southwest to northeast. Moreover, the Δ^{199}Hg values peaked at Lake Tanglha (mean = 0.44‰ ± 0.04‰) before decreased at Lake Qinghai that is under the influence of the westerlies. Our results suggest that transboundary atmospheric transport could transport Hg from South Asia northwards to at least the Tanglha Mountains in the northern Himalaya-Tibet.

Plain Language Summary The fragile ecosystems of the Himalayas and Tibet Plateau region have been suffering transboundary Hg pollution from South Asia. However, the northward extent of this transport of atmospheric Hg pollution remains poorly understood. In our study, sediment core Hg isotope compositions from four lakes (Gokyo, Namco, and Tanglha in the south of the Tanglha Mountains and Qinghai in the north) along a southwest-northeast transect in the region were combined to constrain the northward extent of transboundary Hg pollution by examining both mass-dependent and mass-independent fractionations. Our results suggest that transboundary atmospheric transport could transport Hg from South Asia northwards to at least the Tanglha Mountains in the northern Himalaya-Tibet.

Key Points:

- The δ^{202}Hg signatures among the three lakes in the north are indistinguishable without spatial distribution differences
- Most of sediment samples were characterized by positive Δ^{199}Hg and Δ^{200}Hg values
- The northward extent of atmospheric mercury transboundary transport could be anchored by progressive shifts of Δ^{199}Hg signatures

Supporting Information:

Supporting Information may be found in the online version of this article.

Correspondence to:

S. Kang,
shichang.kang@lzb.ac.cn

Citation:

Huang, J., Kang, S., Feng, X., Tang, W., Ram, K., Guo, J., et al. (2023). Northward extent of atmospheric Mercury transboundary transport to the Himalayas and Tibetan Plateau region. *Geophysical Research Letters*, *50*, e2022GL100948. https://doi.org/10.1029/2022GL100948

Received 31 AUG 2022
Accepted 12 FEB 2023

Author Contributions:

Conceptualization: Jie Huang, Shichang Kang, Feiyue Wang
Formal analysis: Jie Huang
Funding acquisition: Shichang Kang
Methodology: Jie Huang, Shichang Kang, Xinbin Feng, Wenjun Tang, Junming Guo, Qianggong Zhang, Chhatra Mani Sharma, Chaoliu Li, Lekhendra Tripathee
Writing – original draft: Jie Huang, Shichang Kang, Xinbin Feng, Feiyue Wang
Writing – review & editing: Jie Huang, Shichang Kang, Xinbin Feng, Kirpa Ram, Qianggong Zhang, Lekhendra Tripathee, Feiyue Wang

1. Introduction

The Himalayas and Tibetan Plateau region (hereafter, the Himalaya-Tibet) (Figure 1) is home to an extremely remote, isolated, and fragile ecosystem (Yao et al., 2012). With an average altitude of more than 4,000 m a.s.l. and a sparse human population, much of the region has minimal to nonexistent industrial activities. Yet, the Himalaya-Tibet is susceptible to industrial contaminants via long-range atmospheric transport from other regions (Kang et al., 2019). One of the best examples is mercury (Hg), which is a highly toxic global contaminant (AMAP/UNEP, 2018). Rapid economic development in South Asian countries have resulted in considerable releases of Hg into the air (~240 t/yr, or ~10% of the global anthropogenic Hg emissions) (Burger Chakraborty et al., 2013; Mukherjee et al., 2009). The long life time of atmospheric Hg (0.5–1 year for gaseous elemental Hg (GEM); 1–2 weeks for gaseous oxidized Hg (GOM) and particulate bound Hg (Hg_p)) (Schroeder & Munthe, 1998) and the Indian monsoon make it possible for Hg pollution to be transported northwards to and deposited in the Himalaya-Tibet (Huang et al., 2012, 2015). Lake sediments and ice cores retrieved from high elevation of the Himalaya-Tibet could serve as natural archives for documenting the long-term changes of atmospheric Hg. Reconstruction of sediment and ice cores has shown that atmospheric Hg deposition over the Himalaya-Tibet began to rise at the onset of the Industrial Revolution, followed by a dramatic increase after World

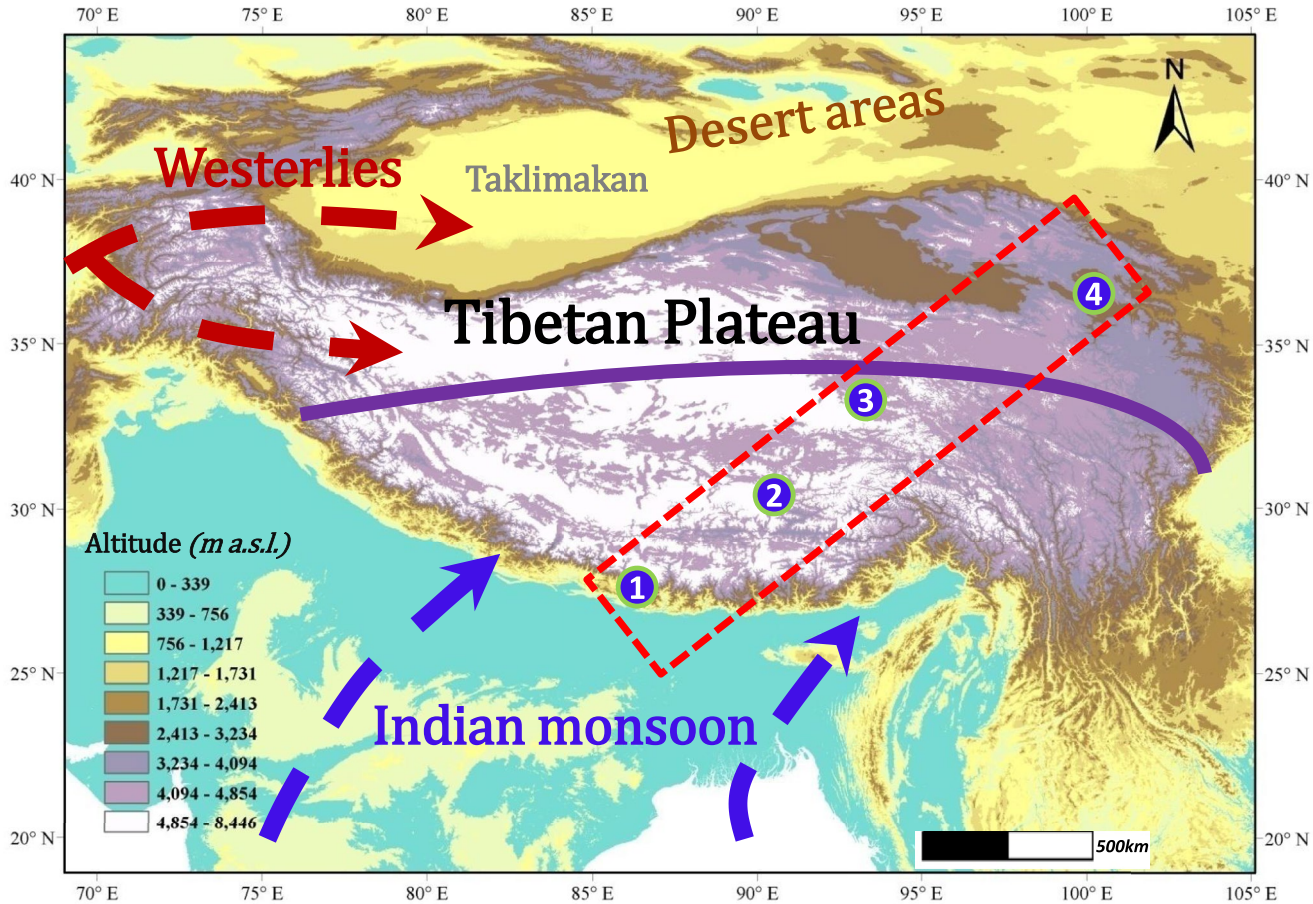

Figure 1. A map of the Himalaya-Tibet, showing locations of Lakes (1) Gokyo, (2) Namco, (3) Tanglha, and (4) Qinghai along a transboundary southwest-northeast transect. Also shown are the general patterns of atmospheric circulation systems. The purple line shows the northern boundary of the India monsoon based on seasonal $\delta^{18}O$ changes in precipitation (Tian et al., 2007), which divides the Himalaya-Tibet into the monsoon-influenced region in the south and the westerlies-influenced region in the north.

War II (Kang et al., 2016), which could be largely attributed to the enhanced anthropogenic perturbations from South Asia (Kang et al., 2019).

Earlier studies have suggested that Indian monsoon intrusion is mainly responsible for the transboundary Hg pollution from South Asia to the Himalaya-Tibet (Huang et al., 2016, Huang, Kang, Yin, Lin, et al., 2020; Kang et al., 2016, 2019; Yu et al., 2022). However, the extent of Indian monsoon influence on atmospheric Hg transport remains unknown. With the breakthrough in Hg isotopic analysis (Bergquist & Blum, 2007), stable Hg isotope geochemistry provides a new tool to address this question, as biogeochemical processes fractionate Hg isotopes differently (both mass-dependent fractionation (MDF, typically measured as $\delta^{202}Hg$) and mass-independent fractionation (MIF, typically measured as $\Delta^{199}Hg$) (Blum & Johnson, 2017; Blum et al., 2014). Recent studies has reported historical changes in Hg isotope compositions from the Himalaya-Tibetan lake sediments (Gokyo (Huang, Kang, Yin, Lin, et al., 2020) Namco and Qinghai (Yin, Feng, et al., 2016)), and linked those changes to variations in Hg sources, pathways and processes (Huang, Kang, Yin, Lin, et al., 2020; Yin, Feng, et al., 2016). For example, $\delta^{202}Hg$ signature overprinting in the Lake Gokyo sediments indicate the Hg source regions from South Asia, and positive $\Delta^{199}Hg$ values in sediments imply that wet Hg deposition is the dominant pathway for sedimentary Hg accumulation (Huang, Kang, Yin, Lin, et al., 2020).

Building on these studies and the measured Hg isotope data from Lake Tanglha (Figure 1), here we explore sediment core Hg isotope compositions from four lakes along a southwest-northeast transect in the region to better understand the northward extent of atmospheric Hg pollution from South Asia. The main objective of our study

was to use Hg isotope signatures to constrain the northward extent of transboundary Hg pollution, which is critically needed for the assessment and management of air pollution in the Himalaya-Tibet. Such information could provide critical insights for more effective mitigation actions on transboundary Hg pollution from South Asia.

2. Materials and Methods

2.1. Study Area and Sediment Coring

The Himalaya-Tibet, known as the "roof of the world," is one of the most imposing topographic features on Earth. The large-scale atmospheric circulation patterns over this region can be generally characterized by the monsoon-influenced region in the south and the westerlies-influenced region in the north (Figure 1).

Four high-altitude lakes were selected to study Hg transboundary transport along a 1,600-km-long transect over the Himalaya-Tibet (Figure 1). They include, from southwest to northeast, Lake Gokyo (4,750 m a.s.l.) in the Gokyo Valley of the Sagarmatha (Everest) National Park, Nepal, in central Himalayas, and Lakes Namco (4,710 m a.s.l.), Tanglha (5,152 m a.s.l.), and Qinghai (3,194 m a.s.l.) on the Tibetan Plateau in China (Table S1 in Supporting Information S1). The distance is ~500 between Gokyo and Namco, ~300 between Namco and Tanglha, and ~800 km between Tanglha and Qinghai.

Sediment cores were retrieved from a deep site of the lakes (~43, 90, 5, and 25 m for Gokyo (retrieved in 2008), Namco (2009), Tanglha (2011), and Qinghai (2006), respectively, using an HTH gravity corer fitted with an 8.5 cm inner diameter polycarbonate tube. The Gokyo (core length: 18.5), Namco (~21), Tanglha (~15), and Qinghai (~7 cm) cores were sectioned at a vertical resolution of 0.5 cm for the upper 1/3 portions and 1 cm for the lower 2/3 portions using a stainless steel slicer. The sediment chronology of the cores was constructed by measuring radionuclide ^{210}Pb, using an ORTEC HPGe GWL series well-type coaxial low background intrinsic germanium detector; the dating results were reported earlier (Kang et al., 2016; X. Wang et al., 2010). A brief introduction of the lakes is provided in Text S1 in Supporting Information S1. More details about the study area, lake properties, and sediment coring can be found elsewhere (Kang et al., 2016; X. Wang et al., 2010; Yin, Feng, et al., 2016).

2.2. Measurement of Isotopic Composition

Hg concentrations and accumulation rates in all the sediment cores (Gokyo, Namco, Tanglha, Qinghai) are briefly presented in Figure S1 and Text S2 in Supporting Information S1 and in details in earlier publications (Kang et al., 2016; X. Wang et al., 2010). Hg isotope compositions of the sediment cores from three of the lakes were also reported earlier: Gokyo (Huang, Kang, Yin, Lin, et al., 2020), and Namco and Qinghai (Yin, Feng, et al., 2016). In this study, Hg isotope compositions of the sediments from Lake Tanglha were analyzed following the methodology described in Yin, Krabbenhoft, et al. (2016). In brief, about 0.2–0.5 g of a freeze-dried sediment sample was digested by 5 mL aqua regia (HCl:HNO_3 = 3:1, v:v) at 95°C for 6 hr in a digestion block. The digested samples were diluted to 0.3–0.5 ng mL^{-1} Hg in 10%–20% aqua regia before isotope analysis on a Neptune-Plus Multi-collector inductively coupled plasma-mass spectrometer (MC-ICP-MS). The certified reference sediment material MESS-1 from National Research Council Canada were digested in the same way and analyzed for quality assurance.

The δ^{202}Hg, Δ^{199}Hg, Δ^{200}Hg, and Δ^{201}Hg values were calculated relative to the Hg standard solution of NIST SRM 3133 (Bergquist & Blum, 2007). For Lake Tanglha, we also analyzed the UM-Almadén as a secondary standard. The results for MESS-1-referenced values (δ^{202}Hg: −1.86‰ ± 0.08‰ (mean ± 2SD); Δ^{199}Hg: 0.01‰ ± 0.04‰; Δ^{200}Hg: 0.01‰ ± 0.02‰; Δ^{201}Hg: −0.02‰ ± 0.04‰; n = 3) and UM-Almadén-referenced values (δ^{202}Hg: −0.52‰ ± 0.08‰; Δ^{199}Hg: −0.01‰ ± 0.03‰; Δ^{200}Hg: 0.00‰ ± 0.02‰; Δ^{201}Hg: −0.02‰ ± 0.03‰; n = 9) were consistent with previous reported values for Lakes Gokyo, Namco, and Qinghai sediments (Huang, Kang, Yin, Lin, et al., 2020; Yin, Feng, et al., 2016).

3. Results and Discussion

3.1. Hg Concentration and Accumulation Rate

The average of Hg concentrations and accumulation rates for the four lake sediment cores are shown in Table S1 in Supporting Information S1. Average Hg concentrations in the lake sediments (range: 18.8–30.5 ng g^{-1};

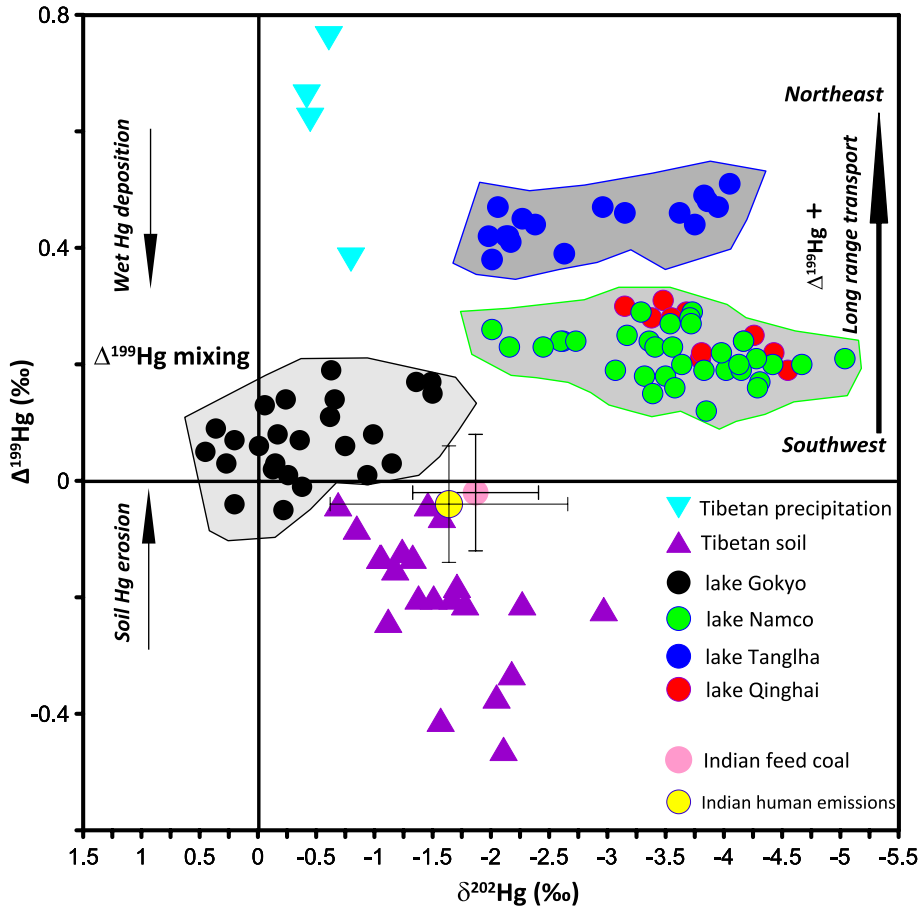

Figure 2. The extent of Hg mass-independent fraction (expressed as Δ^{199}Hg) plotted against that of mass-dependent fractionation (expressed as δ^{202}Hg) in the sediments from Lakes Gokyo (Huang, Kang, Yin, Lin, et al., 2020), Namco (Yin, Feng, et al., 2016), Tanglha (this study), and Qinghai (Yin, Feng, et al., 2016). Hg isotopic compositions in the Tibetan precipitation (Yuan et al., 2015) and soil (X. Wang et al., 2017), and from Indian anthropogenic sources (Das et al., 2016; R. Sun et al., 2014) are also plotted for comparison.

Table S1 in Supporting Information S1) are comparable to those observed in topsoils of the Tibetan Plateau (~37 ng g^{-1}) (Sheng et al., 2012). Averages of sedimentary Hg accumulation rate measured varied from 9.2 ± 7.0 (Qinghai) to 21.9 ± 12.2 μg m^{-2} yr^{-1} (Gokyo), generally decreasing from the southwest (21.9 μg m^{-2} yr^{-1} in Lake Gokyo) that is in close proximity to South Asian Hg source regions to the northeast (9.2 μg m^{-2} yr^{-1} in Qinghai).

3.2. Hg Isotopic Compositions: MDF Records

As shown in Figure 2, sediment samples from the four lakes were generally characterized by negative δ^{202}Hg values (means = −0.42‰ to −3.84‰, $n = 4$), with large variations among the lakes. The δ^{202}Hg values at Gokyo (mean = −0.42‰ ± 0.57‰, 2SD, $n = 25$) were much higher than those at Namco (mean = −3.58‰ ± 0.69‰, 2SD, $n = 34$), Tanglha (mean = −2.77‰ ± 0.78‰, 2SD, $n = 19$), and Qinghai (mean = −3.84‰ ± 0.46‰, 2SD, $n = 11$). In general, the fractionation of anthropogenic Hg isotopes are expected to be less affected during long-range transport from the source regions of South Asia to Lake Gokyo (linear distance ~50 km) when compared to those of Lakes Namco (>500), Tanglha (>800), and Qinghai (>1,600 km) (Figure 1), which have traveled far away from the upwind anthropogenic sources. Therefore, a δ^{202}Hg signature overlapping was found between Lake Gokyo and Indian anthropogenic sources due to its very close proximity to Lake Gokyo (Figure 2), most likely implying the direct input of atmospheric Hg pollution from South Asia.

In contrast, the δ^{202}Hg signatures of Lakes Namco, Tanglha, and Qinghai are markedly different from those of the South Asian sources (Figure 2). The δ^{202}Hg signatures among these three lakes are indistinguishable

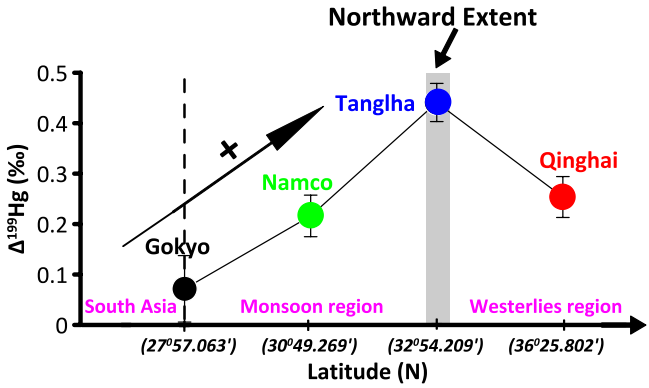

Figure 3. Spatial variations of mean Δ^{199}Hg values in the four lake sediment cores along a transboundary southwest-northeast transect. Data of Hg isotope compositions are available through Huang, Kang, Yin, Lin et al. (2020) (Gokyo sediment core) and Yin, Feng et al. (2016) (Namco and Qinghai sediment cores).

without spatial distribution differences (Figure 2). This could be attributed to the fact that δ^{202}Hg signatures from anthropogenic sources are known to be greatly shifted by many environmental processes during long-range transport including reduction/oxidation, evaporation, volatilization and sorption (Blum et al., 2014). These complicated processes would have resulted in a combined effect on the δ^{202}Hg spatial variations in the sediments of Lakes Namco, Tanglha, and Qinghai (Figure 2). This also makes it difficult to discern the major factors driving the observed differences of δ^{202}Hg variations in our studied lakes at this time.

3.3. Hg Isotopic Compositions: MIF Records

In contrast to Hg-MDF signatures, MIF Hg isotopes are thought to be triggered by photochemical reactions only (Bergquist & Blum, 2007; J. Chen et al., 2012; G. Sun et al., 2016), thus providing a powerful tool to trace atmospheric Hg transport processes. As seen in Figure 2, most of the sediment samples from the four lakes were characterized by positive Δ^{199}Hg values (mean = 0.07‰–0.44‰, $n = 4$). As discussed in the previous studies (Huang, Kang, Yin, Lin, et al., 2020; Yin, Feng, et al., 2016), Hg enters the high-altitude lakes over the Himalaya-Tibet mainly through atmospheric deposition and watershed input of terrestrial soils. Terrestrial soils, which primarily accumulate Hg(0) through litterfall and/or direct deposition of Hg(0), are generally characterized by negative Δ^{199}Hg values (Obrist et al., 2017; X. Wang et al., 2017), while wet scavenging of oxidized/aerosol Hg species from the atmosphere is generally characterized by positive Δ^{199}Hg values (J. Chen et al., 2012; Z. Wang et al., 2015; Yuan et al., 2015). The geogenic Hg sources such as chemical weathering are generally characterized by zero Δ^{199}Hg value due to the lack of photochemical reactions (Blum et al., 2014). As most sediment samples are characterized by positive Δ^{199}Hg values (Figure 2), it is deduced that atmospheric Hg deposition through precipitation appears to play a more important pathway for sedimentary Hg accumulation. Our earlier studies have implied that Hg in sediments from Gokyo, Namco, and Qinghai is derived predominantly from atmospheric wet Hg deposition with positive Δ^{199}Hg values (Huang, Kang, Yin, Lin, et al., 2020; Yin, Feng, et al., 2016). Large positive Δ^{199}Hg values were also observed in the sediments of Lake Tanglha in this study (Figure 2), confirming the important role of atmospheric Hg deposition through precipitation. MIF of even-mass Hg isotopes has been widely observed in environmental samples generally with positive Δ^{200}Hg in precipitation (J. Chen et al., 2012; Gratz et al., 2010), though the mechanism for MIF of ^{200}Hg remains unclear (Blum et al., 2014; Cai & Chen, 2016). Most of the Δ^{200}Hg in sediment samples were characterized by small positive values (Gokyo, mean = 0.03‰ ± 0.04‰; Namco, mean = 0.06‰ ± 0.01‰; Tanglha, mean = 0.04‰ ± 0.02‰; Qinghai, mean = 0.08‰ ± 0.01‰), further supporting the importance of wet Hg deposition in our study area.

More importantly, our results show large variations of Hg-MIF signatures along the transboundary southwest-northeast transect. As shown in Figure 3, there is an increasing trend of positive Δ^{199}Hg values from Gokyo (mean = 0.07‰ ± 0.06‰, 2SD, $n = 25$) to Tanglha (mean = 0.44‰ ± 0.04‰, 2SD, $n = 19$) except for Qinghai (mean = 0.25‰ ± 0.04‰, 2SD, $n = 11$) (more discussion below). A recent compilation of Hg isotopic signatures has demonstrated that atmospheric Hg emitted from anthropogenic sources worldwide is generally characterized by average Δ^{199}Hg values of −0.06‰ to −0.04‰ (R. Y. Sun et al., 2016). Similarly, a previous study in industrialized and urbanized Kolkata in Northeastern India has reported near zero Δ^{199}Hg values in air (Das et al., 2016). This is consistent with the observed Δ^{199}Hg (mean = 0.07‰) in the Gokyo sediments (Figure 2), indicating that strong anthropogenic emissions from South Asia drive Hg isotopic composition toward low Δ^{199}Hg values. In contrast, Δ^{199}Hg values of most sediment samples in the other three lakes (mean = 0.29‰, 2SD, $n = 64$) are more largely positive than anthropogenic emissions (close to zero Δ^{199}Hg value) (Figures 2 and 3) (Das et al., 2016; R. Sun et al., 2014), indicating important roles of atmospheric transformations.

Atmospheric Hg_P could be derived from anthropogenic emission sources and/or produced from the oxidation of GEM on particulate surfaces and in gas phase followed by gas-particle partitioning (Amos et al., 2012; Ariya et al., 2015). In the monsoon-influenced region, the latter is expected to have a lesser effect on atmospheric HgP concentrations for several reasons: (a) increased precipitation during the monsoon period could effectively

remove atmospheric particulates, resulting in lower concentrations of particulate matter in the air; (b) the widespread glacier and snow cover exist in the monsoon-influenced region (Yao et al., 2019) may hamper particulate emissions from the surface soil, and the formations of snow or ice crystals in the cryospheric environments could facilitate the scavenging of atmospheric Hg (Douglas & Blum, 2019; Douglas et al., 2008); and (c) the monsoon climate in cold Himalaya-Tibet could further restrict particulate emissions from the cold and wet surface (Yao et al., 2019). This is supported by the extremely low dust emissions (~29 Tg yr^{-1}, S. Chen et al., 2014) in the Himalaya-Tibet, which is about ~8% of natural dust emissions from arid desert areas in the westerlies-influenced region (~367 Tg yr^{-1}, S. Chen et al., 2017). The extremely high atmospheric Hg_P concentrations have been reported in South Asia (e.g., 159–408 pg m^{-3}, Kolkata, India (Das et al., 2016); 120–1,855 pg m^{-3}, Kathmandu, Nepal (Guo et al., 2017, 2021)), supporting anthropogenic emissions from South Asia could be the main sources of atmospheric HgP to the Himalaya-Tibet.

Numerous studies from the Himalaya-Tibet have suggested that atmospheric Hg deposition is primarily associated with particulate matter (Loewen et al., 2007; Q. Zhang et al., 2012), and HgP is the dominant form of Hg in precipitation (~78.4%, Huang et al., 2022). Below-cloud scavenging of HgP is thus an important mechanism contributing atmospheric Hg to wet deposition (Huang et al., 2012, 2013). These findings further support that the transboundary-transported HgP could be the primary source to our studied lake sediments. As shown in Figure S2 in Supporting Information S1, sediments from the four lakes yield a slope of 0.99 for the $\Delta^{199}Hg/\Delta^{201}Hg$ ratio, which is consistent with the value reported during aqueous Hg(II) photoreduction (Blum et al., 2014). Photoreduction of Hg(II) in atmospheric particulate matter is thus most likely responsible for the positive $\Delta^{199}Hg$ values at our study sites (Bergquist & Blum, 2007; K. Zhang et al., 2022; Zheng & Hintelmann, 2009).

Previous studies have demonstrated that anthropogenic pollution plumes from South Asia need to travel a long time (several days) before arriving to northern part of the Himalaya-Tibet (Lüthi et al., 2015; Xia et al., 2011), and a significant fraction of atmospheric HgP is lost via photoreductions during long-range transport (Fu et al., 2019). These processes would have facilitated atmospheric HgP transformations with a significant positive shift of $\Delta^{199}Hg$ in atmospheric HgP, given the dramatic MIF factors induced by photochemical reduction as determined by previous experiments (Bergquist & Blum, 2007). Thus, atmospheric Hg_P to the northwest would have undergone more extensive photochemical reduction before being scavenged in wet precipitation (Figure 2), which could explain the more positive $\Delta^{199}Hg$ values in northern lake sediments (Figure 3).

It should be noted, however, that atmospheric Hg_P in our study area might also be affected by atmospheric transport processes that could affect the Hg MIF signatures (e.g., photoreduction of gas-phase Hg(II)), the mechanisms of which remain poorly understood (Cai & Chen, 2016; Fu et al., 2019; Saiz-Lopez et al., 2018). Moreover, several important environmental processes within the lake could also influence the $\Delta^{199}Hg$ isotopic compositions in the lake sediment. Some of these processes include transformations of Hg in water column (e.g., Kurz et al., 2019; Motta et al., 2019), bioaccumulation and biomass depositions in aquatic system (Kwon et al., 2020; Tsui et al., 2020), biologically influenced Hg morphological transformation (Ridley & Stetson, 2006; Yin et al., 2014) as well as formation and melting of the seasonal lake ice cover in aquatic system (Masbou et al., 2015; Point et al., 2011) and the isotopic compositions of legacy of Hg through remobilization in lake catchment (Janssen et al., 2021; R. Sun et al., 2022). For example, the transformations of Hg in water column may be expected to have less effect on our MIF-Hg signatures because of the shallow lake water depths (e.g., ~5 m in Lake Tanglha) in our lake deposits. This could facilitate a rapid settlement of atmospheric Hg_P deposition and conservation of the $\Delta^{199}Hg$ isotopic compositions from atmospheric Hg source (Lepak et al., 2015). Unfortunately, the extent and relative importance of most of these environmental processes on the isotopic compositions are unknown at this time due to the lack of data, and more studies on potential processes affecting the MIF-Hg isotopes in lake sediment are needed.

3.4. Northward Extent of Atmospheric Hg Transboundary Transport

On the basis of the presumed lack of $\Delta^{199}Hg$ fractionation during above-mentioned environmental processing, $\Delta^{199}Hg$ values in lake sediments may provide a new tool to determine the northward extent of atmospheric Hg transboundary transport from South Asia. As shown in Figure 3, the $\Delta^{199}Hg$ values in lake sediments increase progressively with distance from southwest to northeast, peaked at Lake Tanglha, before at Lake Qinghai. Previous studies based on seasonal $\delta^{18}O$ changes have suggested that the Tanglha Mountains (~34°–35°N) in the northern Himalaya-Tibet Plateau is the northward maximum extent of Indian monsoon penetration (Figure 1)

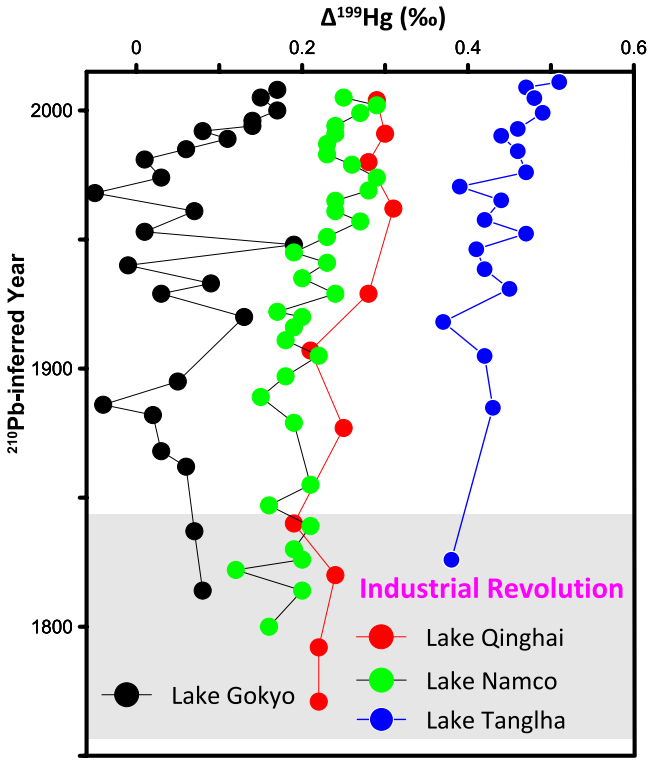

Figure 4. Historical changes of Δ^{199}Hg values in the profiles of the sediment cores from the Lakes Gokyo, Namco, Tanglha, and Qinghai. Gray bar represents the Industrial Revolution period. Data of Hg isotope compositions are available through Huang, Kang, Yin, Lin et al. (2020) (Gokyo sediment core) and Yin, Feng et al. (2016) (Namco and Qinghai sediment cores).

(Tian et al., 2007). As Lake Tangla is located at ~33°N, and Lake Qinghai ~36.5°N, our results not only support this northward maximum extent of Indian monsoon, but also establish that Hg originated from South Asia can be transported northwards up to the Tanglha Mountains.

The decrease in Δ^{199}Hg values in sediments of Lake Qinghai is due to the influence of the westerlies instead of the Indian monsoon. The upwind anthropogenic Hg source of Lake Qinghai are in European and Central Asian countries that have shown a significant decreasing trend of anthropogenic Hg emissions during the past several decades (Muntean et al., 2018; J. M. Pacyna et al., 2009). Its impact on the Δ^{199}Hg values of Lake Qinghai sediments is thus much smaller than that of the South Asian Hg sources on the other three lakes. Instead, the lower Δ^{199}Hg values in sediments of Lake Qinghai suggest the dominance of natural Hg sources from the vast desert and semidesert areas to its west (Figure 1). This region produces enormous amount of dust (~367 Tg/yr, S. Chen et al., 2017) which is characterized by high atmospheric HgP concentrations (e.g., ~250 pg m^{-3} in the Taklimakan Desert; Huang, Kang, Yin, Ram, et al., 2020), resulting in a total atmospheric HgP flux of ~60 Mg/yr (Huang, Kang, Yin, Ram, et al., 2020). Dust-sourced Hg_P is known to have lower Δ^{199}Hg values (Fu et al., 2019), which would explain the drop in Δ^{199}Hg values in the sediments from Lake Qinghai. Whereas a significant correlation is found between Hg concentrations and Δ^{199}Hg values in sediments from Lakes Gokyo, Namco, and Tanglha ($p < 0.05$), the correlation is insignificant in Lake Qinghai ($p = 0.15$) (Figure S3 in Supporting Information S1), further supporting that Lake Qinghai is influenced by different Hg sources and processes than the other three lakes.

3.5. Summary and Implications

It has been shown that Indian monsoon intrusion drives intensive anthropogenic Hg emissions from South Asia to the Himalaya-Tibet (Kang et al., 2016, 2019), and that wet scavenging of atmospheric Hg by monsoon precipitation is an important pathway for Hg accumulation in lake sediments in the region (Huang, Kang, Yin, Lin, et al., 2020). By examining Hg isotopic compositions in lake sediments, our study shows that the northward extent of transboundary Hg pollution from South Asia could reach the Tanglha Mountains in the northern Himalaya-Tibet (Figure S4 in Supporting Information S1). Moreover, positive shifts of Hg-MIF signatures along this transect appeared since the Industrial Revolution (Figure 4), indicating that such transboundary Hg pollution has been operating since then. Since anthropogenic Hg emissions from South Asia are projected to increase despite the Minamata Convention (E. G. Pacyna et al., 2010; Streets et al., 2009), and precipitation in the monsoon-influenced region is projected to increase (by ~10% in 2015–2050 relative to 1961–1990; D. Chen et al., 2015), the loadings of Hg to the southern Himalaya-Tibet region will likely further increase. Although our study suggests that the Himalaya-Tibet region acts as a receptor site for the transboundary Hg pollution from South Asia through Indian monsoon, several important environmental processes such as bioaccumulation, biomass depositions and transformations of Hg within the water column as well as weathering of soil and their isotopic compositions can significantly influence Hg budget in the lake sediments. Therefore, more Hg isotope data are required to establish our preliminary findings on transboundary transport in southwest-northeast transect and to better understand the sources and processes affecting isotopic compositions and Hg budget in the lake sediments. Further studies are also needed to better assess how the fragile alpine and cryospheric ecosystems would respond to such increases in transboundary transport of Hg from South Asia in a changing climate.

Data Availability Statement

Supporting data for Hg isotope compositions in the Lake Tanglha sediment core available from https://doi.org/10.7910/DVN/9YFDML.

Acknowledgments
This study was supported by the Second Tibetan Plateau Scientific Expedition and Research Program (STEP) (2019QZKK0605), the Pan-Third Pole Environment Study for a Green Silk Road (Pan-TPE) (XDA20040500), the National Natural Science Foundation of China (42277397, 41977335, and 41421061), the Foundation of State Key Laboratory of Cryospheric Science, CAS (SKLCS-ZZ-2022). F.W. acknowledges the support from the Canada Research Chairs Program. KR thanks Banaras Hindu University for granting the study leave and CAS for international visiting scientist support under the PIFI (2018VCC0005). We would like to acknowledge and thank Dr. Wang Zheng and Dr. Hongming Cai for providing helpful comments on an earlier version of this manuscript.

References

AMAP/UNEP. (2018). *Technical background assessment for the 2018 global Mercury assessment*. United Nations Environment Programme.
Amos, H. M., Jacob, D. J., Holmes, C. D., Fisher, J. A., Wang, Q., Yantosca, R. M., et al. (2012). Gas particle partitioning of atmospheric Hg(II) and its effect on global Mercury deposition. *Atmospheric Chemistry and Physics*, *12*(1), 591–603. https://doi.org/10.5194/acp-12-591-2012
Ariya, P. A., Amyot, M., Dastoor, A., Deeds, D., Feinberg, A., Kos, G., et al. (2015). Mercury physicochemical and biogeochemical transformation in the atmosphere and at atmospheric interfaces: A review and future directions. *Chemical Reviews*, *115*(10), 3760–3802. https://doi.org/10.1021/cr500667e
Bergquist, B. A., & Blum, J. D. (2007). Mass-dependent and-independent fractionation of Hg isotopes by photoreduction in aquatic systems. *Science*, *318*(5849), 417–420. https://doi.org/10.1126/science.1148050
Blum, J. D., & Johnson, M. W. (2017). Recent developments in Mercury stable isotope analysis. *Reviews in Mineralogy and Geochemistry*, *82*(1), 733–757. https://doi.org/10.2138/rmg.2017.82.17
Blum, J. D., Sherman, L. S., & Johnson, M. W. (2014). Mercury isotopes in Earth and environmental sciences. *Annual Review of Earth and Planetary Sciences*, *42*(1), 249–269. https://doi.org/10.1146/annurev-earth-050212-124107
Burger Chakraborty, L., Qureshi, A., Vadenbo, C., & Hellweg, S. (2013). Anthropogenic mercury flows in India and impacts of emission controls. *Environmental Science & Technology*, *47*, 8105–8113. https://doi.org/10.1021/es401006k
Cai, H., & Chen, J. (2016). Mass-independent fractionation of even Mercury isotopes. *Science Bulleti*n, *61*(2), 116–124. https://doi.org/10.1007/s11434-015-0968-8
Chen, D., Xu, B., Yao, T., Guo, Z., Cui, P., Chen, F., et al. (2015). Assessment of past, present and future environmental changes on the Tibetan Plateau. *Chinese Science Bulletin*, *60*(32), 3025–3035.
Chen, J., Hintelmann, H., Feng, X., & Dimock, B. (2012). Unusual fractionation of both odd and even mercury isotopes in precipitation from Peterborough, ON, Canada. *Geochimica et Cosmochimica Acta*, *90*, 33–46. https://doi.org/10.1016/j.gca.2012.05.005
Chen, S., Huang, J., Li, J., Jia, R., Jiang, N., Kang, L., et al. (2017). Comparison of dust emissions, transport, and deposition between the Taklimakan Desert and Gobi desert from 2007 to 2011. *Science China Earth Sciences*, *60*(7), 1338–1355. https://doi.org/10.1007/s11430-016-9051-0
Chen, S., Zhao, C., Qian, Y., Leung, L. R., Huang, J., Huang, Z., et al. (2014). Regional modeling of dust mass balance and radiative forcing over East Asia using WRF-Chem. *Aeolian Research*, *15*, 15–30. https://doi.org/10.1016/j.aeolia.2014.02.001
Das, R., Wang, X., Khezri, B., Webster, R. D., Sikdar, P. K., & Datta, S. (2016). Mercury isotopes of atmospheric particle bound Mercury for source apportionment study in urban Kolkata, India. *Elementa: Science of the Anthropocene*, *4*, 000098. https://doi.org/10.12952/journal.elementa.000098
Douglas, T. A., & Blum, J. D. (2019). Mercury isotopes reveal atmospheric gaseous Mercury deposition directly to the Arctic coastal snowpack. *Environmental Science & Technology Letters*, *6*(4), 235–242. https://doi.org/10.1021/acs.estlett.9b00131
Douglas, T. A., Sturm, M., Simpson, W. R., Blum, J. D., Alvarez-Aviles, L., Keeler, G. J., et al. (2008). Influence of snow and ice crystal formation and accumulation on Mercury deposition to the Arctic. *Environmental Science & Technology*, *42*(5), 1542–1551. https://doi.org/10.1021/es070502d
Fu, X., Zhang, H., Feng, X., Tan, Q., Ming, L., Liu, C., & Zhang, L. (2019). Domestic and transboundary sources of atmospheric particulate bound mercury in remote areas of China: Evidence from Mercury isotopes. *Environmental Science & Technology*, *53*(4), 1947–1957. https://doi.org/10.1021/acs.est.8b06736
Gratz, L. E., Keeler, G. J., Blum, J. D., & Sherman, L. S. (2010). Isotopic composition and fractionation of Mercury in Great Lakes precipitation and ambient air. *Environmental Science & Technology*, *44*(20), 7764–7770. https://doi.org/10.1021/es100383w
Guo, J., Kang, S., Huang, J., Zhang, Q., Rupakheti, M., Sun, S., et al. (2017). Characterizations of atmospheric particulate-bound mercury in the Kathmandu Valley of Nepal, South Asia. *Science of the Total Environment*, *579*, 1240–1248. https://doi.org/10.1016/j.scitotenv.2016.11.110
Guo, J., Sharma, C. M., Tripathee, L., Kang, S., Fu, X., Huang, J., et al. (2021). Source identification of atmospheric particle-bound mercury in the Himalayan foothills through non-isotopic and isotope analyses. *Environmental Pollution*, *286*, 117317. https://doi.org/10.1016/j.envpol.2021.117317
Huang, J., Kang, S., Tian, L., Guo, J., Zhang, Q., Cong, Z., et al. (2016). Influence of long-range transboundary transport on atmospheric water vapor mercury collected at the largest city of Tibet. *Science of the Total Environment*, *566–567*, 1215–1222. https://doi.org/10.1016/j.scitotenv.2016.05.177
Huang, J., Kang, S., Wang, L., Liu, K., Ram, K., Sillanpää, M., et al. (2022). Anthropogenic and natural drivers of seesaw-like spatial patterns in precipitation Mercury over western China. *Environmental Pollution*, *307*, 119525. https://doi.org/10.1016/j.envpol.2022.119525
Huang, J., Kang, S., Wang, S., Wang, L., Zhang, Q., Guo, J., et al. (2013). Wet deposition of mercury at Lhasa, the capital city of Tibet. *Science of the Total Environment*, *447*, 123–132. https://doi.org/10.1016/j.scitotenv.2013.01.003
Huang, J., Kang, S., Yin, R., Lin, M., Guo, J., Ram, K., et al. (2020). Decoupling natural and anthropogenic Mercury and lead transport from South Asia to the Himalayas. *Environmental Science & Technology*, *54*(9), 5429–5436. https://doi.org/10.1021/acs.est.0c00429
Huang, J., Kang, S., Yin, R., Ram, K., Liu, X., Lu, H., et al. (2020). Desert dust as a significant carrier of atmospheric Mercury. *Environmental Pollution*, *267*, 115442. https://doi.org/10.1016/j.envpol.2020.115442
Huang, J., Kang, S., Zhang, Q., Guo, J., Sillanpää, M., Wang, Y., et al. (2015). Characterizations of wet mercury deposition on a remote high-elevation site in the southeastern Tibetan Plateau. *Environmental Pollution*, *206*, 518–526. https://doi.org/10.1016/j.envpol.2015.07.024
Huang, J., Kang, S., Zhang, Q., Yan, H., Guo, J., Jenkins, M. G., et al. (2012). Wet deposition of mercury at a remote site in the Tibetan Plateau: Concentrations, speciation, and fluxes. *Atmospheric Environment*, *62*, 540–550. https://doi.org/10.1016/j.atmosenv.2012.09.003
Janssen, S. E., Tate, M. T., Krabbenhoft, D. P., DeWild, J. F., Ogorek, J. M., Babiarz, C. L., et al. (2021). The influence of legacy contamination on the transport and bioaccumulation of mercury within the Mobile River Basin. *Journal of Hazardous Materials*, *404*, 124097. https://doi.org/10.1016/j.jhazmat.2020.124097
Kang, S., Huang, J., Wang, F., Zhang, Q., Zhang, Y., Li, C., et al. (2016). Atmospheric mercury depositional chronology reconstructed from lake sediments and ice core in the Himalayas and Tibetan Plateau. *Environmental Science & Technology*, *50*(6), 2859–2869. https://doi.org/10.1021/acs.est.5b04172
Kang, S., Zhang, Q., Qian, Y., Ji, Z., Li, C., Cong, Z., et al. (2019). Linking atmospheric pollution to cryospheric change in the third Pole region: Current progress and future prospects. *National Science Review*, *6*(4), 796–809. https://doi.org/10.1093/nsr/nwz031
Kurz, A. Y., Blum, J. D., Washburn, S. J., & Baskaran, M. (2019). Changes in the mercury isotopic composition of sediments from a remote alpine lake in Wyoming, USA. *Science of the Total Environment*, *669*, 973–982. https://doi.org/10.1016/j.scitotenv.2019.03.165
Kwon, S. Y., Blum, J. D., Yin, R., Tsui, M. T. K., Yang, Y. H., & Choi, J. W. (2020). Mercury stable isotopes for monitoring the effectiveness of the Minamata convention on Mercury. *Earth-Science Reviews*, *203*, 103111. https://doi.org/10.1016/j.earscirev.2020.103111

Lepak, R. F., Yin, R., Krabbenhoft, D. P., Ogorek, J. M., DeWild, J. F., Holsen, T. M., & Hurley, J. P. (2015). Use of stable isotope signatures to determine mercury sources in the Great Lakes. *Environmental Science & Technology Letters*, *2*(12), 335–341. https://doi.org/10.1021/acs.estlett.5b00277

Loewen, M., Kang, S., Armstrong, D., Zhang, Q., Tomy, G., & Wang, F. (2007). Atmospheric transport of Mercury to the Tibetan Plateau. *Environmental Science & Technology*, *41*(22), 7632–7638. https://doi.org/10.1021/es0710398

Lüthi, Z., Škerlak, B., Kim, S., Lauer, A., Mues, A., Rupakheti, M., & Kang, S. (2015). Atmospheric Brown clouds reach the Tibetan Plateau by crossing the Himalayas. *Atmospheric Chemistry and Physics*, *15*(11), 1–15. https://doi.org/10.5194/acp-15-6007-2015

Masbou, J., Point, D., Sonke, J. E., Frappart, F., Perrot, V., Amouroux, D., et al. (2015). Hg stable isotope time trend in ringed seals registers decreasing sea ice cover in the Alaskan Arctic. *Environmental Science & Technology*, *49*(15), 8977–8985. https://doi.org/10.1021/es5048446

Motta, L. C., Blum, J. D., Johnson, M. W., Umhau, B. P., Popp, B. N., Washburn, S. J., et al. (2019). Mercury cycling in the north Pacific subtropical gyre as revealed by Mercury stable isotope ratios. *Global Biogeochemical Cycles*, *33*(6), 777–794. https://doi.org/10.1029/2018gb006057

Mukherjee, A. B., Bhattacharya, P., Sarkar, A., Zevenhoven, R., & Bodaly (2009). *Mercury emissions from industrial sources in India and its effects in the environment* (pp. 81–112). Springer. Chap. 4.

Muntean, M., Janssens-Maenhout, G., Song, S., Giang, A., Selin, N. E., Zhong, H., et al. (2018). Evaluating EDGARv4.tox2 speciated mercury emissions ex-post scenarios and their impacts on modelled global and regional wet deposition patterns. *Atmospheric Environment*, *184*, 56–68. https://doi.org/10.1016/j.atmosenv.2018.04.017

Obrist, D., Agnan, Y., Jiskra, M., Olson, C. L., Colegrove, D. P., Hueber, J., et al. (2017). Tundra uptake of atmospheric elemental Mercury drives Arctic Mercury pollution. *Nature*, *547*(7662), 201–204. https://doi.org/10.1038/nature22997

Pacyna, E. G., Pacyna, J., Sundseth, K., Munthe, J., Kindbom, K., Wilson, S., et al. (2010). Global emission of Mercury to the atmosphere from anthropogenic sources in 2005 and projections to 2020. *Atmospheric Environment*, *44*(20), 2487–2499. https://doi.org/10.1016/j.atmosenv.2009.06.009

Pacyna, J. M., Pacyna, E. G., & Aas, W. (2009). Changes of emissions and atmospheric deposition of Mercury, lead, and cadmium. *Atmospheric Environment*, *43*(1), 117–127. https://doi.org/10.1016/j.atmosenv.2008.09.066

Point, D., Sonke, J. E., Day, R. D., Roseneau, D. G., Hobson, K. A., Vander Pol, S. S., et al. (2011). Methylmercury photodegradation influenced by sea-ice cover in Arctic marine ecosystems. *Nature Geoscience*, *4*(3), 188–194. https://doi.org/10.1038/ngeo1049

Ridley, W. I., & Stetson, S. J. (2006). A review of isotopic composition as an indicator of the natural and anthropogenic behavior of Mercury. *Applied Geochemistry*, *21*(11), 1889–1899. https://doi.org/10.1016/j.apgeochem.2006.08.006

Saiz-Lopez, A., Sitkiewicz, S. P., Roca-Sanjuán, D., Oliva-Enrich, J. M., Dávalos, J. Z., Notario, R., et al. (2018). Photoreduction of gaseous oxidized mercury changes global atmospheric Mercury speciation, transport and deposition. *Nature Communications*, *9*(1), 4796. https://doi.org/10.1038/s41467-018-07075-3

Schroeder, W. H., & Munthe, J. (1998). Atmospheric Mercury-an overview. *Atmospheric Environment*, *32*(5), 809–822. https://doi.org/10.1016/s1352-2310(97)00293-8

Sheng, J., Wang, X., Gong, P., Tian, L., & Yao, T. (2012). Heavy metals of the Tibetan top soils. *Environmental Science & Pollution Research*, *19*(8), 3362–3370. https://doi.org/10.1007/s11356-012-0857-5

Streets, D. G., Zhang, Q., & Wu, Y. (2009). Projections of global Mercury emissions in 2050. *Environmental Science & Technology*, *43*(8), 2983–2988. https://doi.org/10.1021/es802474j

Sun, G., Sommar, J., Feng, X., Lin, C.-J., Ge, M., Wang, W., et al. (2016). Mass-dependent and -independent fractionation of mercury isotope during gas-phase oxidation of elemental mercury vapor by atomic Cl and Br. *Environmental Science & Technology*, *50*(17), 9232–9241. https://doi.org/10.1021/acs.est.6b01668

Sun, R., Hintelmann, H., Wiklund, J. A., Evans, M. S., Muir, D., & Kirk, J. L. (2022). Mercury isotope variations in lake sediment cores in response to direct mercury emissions from non-ferrous metal smelters and legacy Mercury remobilization. *Environmental Science & Technology*, *56*(12), 8266–8277. https://doi.org/10.1021/acs.est.2c02692

Sun, R., Sonke, J. E., Heimbürger, L. E., Belkin, H. E., Liu, G., Shome, D., et al. (2014). Mercury stable isotope signatures of world coal deposits and historical coal combustion emissions. *Environmental Science & Technology*, *48*(13), 7660–7668. https://doi.org/10.1021/es501208a

Sun, R. Y., Streets, D. G., Horowitz, H. M., Amos, H. M., Liu, G. J., Perrot, V., et al. (2016). Historical (1850–2010) Mercury stable isotope inventory from anthropogenic sources to the atmosphere. *Elementa: Science of the Anthropocene*, *4*(91), 000091. https://doi.org/10.12952/journal.elementa.000091

Tian, L., Yao, T., MacClune, K., White, J. W. C., Schilla, A., Vaughn, B., et al. (2007). Stable isotopic variations in west China: A consideration of moisture sources. *Journal of Geophysical Research*, *112*(D10), D10112. https://doi.org/10.1029/2006jd007718

Tsui, M. T. K., Blum, J. D., & Kwon, S. Y. (2020). Review of stable Mercury isotopes in ecology and biogeochemistry. *Science of the Total Environment*, *716*, 135386. https://doi.org/10.1016/j.scitotenv.2019.135386

Wang, X., Luo, J., Yin, R., Yuan, W., Lin, C. J., Sommar, J., et al. (2017). Using mercury isotopes to understand Mercury accumulation in the montane forest floor of the eastern Tibetan Plateau. *Environmental Science & Technology*, *51*(2), 801–809. https://doi.org/10.1021/acs.est.6b03806

Wang, X., Yang, H., Gong, P., Zhao, X., Wu, G., Turner, S., et al. (2010). One century sedimentary records of polycyclic aromatic hydrocarbons, mercury and trace elements in the Qinghai Lake, Tibetan Plateau. *Environmental Pollution*, *158*(10), 3065–3070. https://doi.org/10.1016/j.envpol.2010.06.034

Wang, Z., Chen, J., Feng, X., Hintelmann, H., Yuan, S., Cai, H., et al. (2015). Mass-dependent and mass-independent fractionation of Mercury isotopes in precipitation from Guiyang, SW China. *Comptes Rendus Geoscience*, *347*(7–8), 358–367. https://doi.org/10.1016/j.crte.2015.02.006

Xia, X., Zong, X., Cong, Z., Chen, H., Kang, S., & Wang, P. (2011). Baseline continental aerosol over the central Tibetan Plateau and a case study of aerosol transport from South Asia. *Atmospheric Environment*, *45*(39), 7370–7378. https://doi.org/10.1016/j.atmosenv.2011.07.067

Yao, T., Thompson, L. G., Mosbrugger, V., Zhang, F., Ma, Y., Luo, T., et al. (2012). Third Pole environment (TPE). *Environmental Development*, *3*, 52–64. https://doi.org/10.1016/j.envdev.2012.04.002

Yao, T., Xue, Y., Chen, D., Chen, F., Thompson, L., Cui, P., et al. (2019). Recent third Pole's rapid warming accompanies cryospheric melt and water cycle intensification and interactions between monsoon and environment: Multidisciplinary approach with observations, modeling, and analysis. *Bulletin of the American Meteorological Society*, *100*(3), 423–444. https://doi.org/10.1175/bams-d-17-0057.1

Yin, R., Feng, X., Hurley, J. P., Krabbenhoft, D. P., Lepak, R. F., Kang, S., et al. (2016). Historical records of Mercury stable isotopes in sediments of Tibetan lakes. *Scientific Reports*, *6*(1), 23332. https://doi.org/10.1038/srep23332

Yin, R., Feng, X., Li, X., Yu, B., & Du, B. (2014). Trends and advances in Mercury stable isotopes as a geochemical tracer. *Trends in Analytical Chemistry*, *2*, 1–10. https://doi.org/10.1016/j.teac.2014.03.001

Yin, R., Krabbenhoft, D. P., Bergquist, B. A., Zheng, W., Lepak, R. F. & Hurley, J. P. (2016). Effects of mercury and thallium concentrations on high precision determination of mercury isotopic composition by Neptune Plus multiple collector inductively coupled plasma mass spectrometry. *Journal of Analytical Atomic Spectrometry*, *31*(10), 2060–2068. https://doi.org/10.1039/c6ja00107f

Yu, B., Yang, L., Liu, H., Xiao, C., Bu, D., Zhang, Q., et al. (2022). Tracing the transboundary transport of Mercury to the Tibetan Plateau using atmospheric Mercury isotopes. *Environmental Science & Technology*, *56*(3), 1568–1577. https://doi.org/10.1021/acs.est.1c05816

Yuan, S., Zhang, Y., Chen, J., Kang, S., Zhang, J., Feng, X., et al. (2015). Large variation of Mercury isotope composition during a single precipitation event at Lhasa City, Tibetan Plateau, China. *Procedia Earth and Planetary Science*, *13*, 282–286. https://doi.org/10.1016/j.proeps.2015.07.066

Zhang, K., Zheng, W., Sun, R., He, S., Shuai, W., Fan, X., et al. (2022). Stable isotopes reveal photoreduction of particle-bound mercury driven by water-soluble organic carbon during severe haze. *Environmental Science & Technology*, *56*(15), 10619–10628. https://doi.org/10.1021/acs.est.2c01933

Zhang, Q., Huang, J., Wang, F., Loewen, M., Xu, J., Armstrong, D., et al. (2012). Mercury distribution and deposition in glacier snow over western China. *Environmental Science & Technology*, *46*(10), 5404–5413. https://doi.org/10.1021/es300166x

Zheng, W., & Hintelmann, H. (2009). Mercury isotope fractionation during photoreduction in natural water is controlled by its Hg/DOC ratio. *Geochimica et Cosmochimica Acta*, *73*(22), 6704–6715. https://doi.org/10.1016/j.gca.2009.08.016